

## The Electrochemical Behavior of 15-5PH Stainless Steel in Acidic Solutions

Q. Yu<sup>1,2</sup>, C.F. Dong<sup>1,\*</sup>, Z.B. Liu<sup>2</sup>, J.X. Liang<sup>2</sup>, K. Xiao<sup>1</sup>, X.G. Li<sup>1</sup>

<sup>1</sup> Corrosion and Protection Center, Institute of Advanced Materials and Technology, University of Science and Technology Beijing, Beijing 100083, China

<sup>2</sup> Institute for special steel central Iron and steel Research Institute, Beijing 100081, China

\* E-mail: [cfdong@ustb.edu.cn](mailto:cfdong@ustb.edu.cn)

Received: 27 November 2014 / Accepted: 31 December 2014 / Published: 19 January 2015

---

In this paper, the potentiodynamic polarization and electrochemical impedance spectroscopy (EIS) of 15-5PH stainless steel were measured in the 0.5M Na<sub>2</sub>SO<sub>4</sub> acid solution with various pH values and Cl<sup>-</sup> concentrations. The characteristics of surface passive film formed under different corrosive conditions were analyzed using X-ray photoelectron spectroscopy (XPS). It is found that all the polarization curves of 15-5PH steel present passivity in the testing acid solution, and the corrosion current density change from 16.032 μA to 1.967 μA with the pH value increasing between 1 and 5. In contrast to the current performance, the impedance changed oppositely. With addition of Cl<sup>-</sup> the pits initiated on the steel electrode and the pitting potential was reduced by increasing concentration of Cl<sup>-</sup>. Moreover, the oxides and hydroxides of Fe, Cr, Ni and Cu are the primary components of the passive film.

---

**Keywords:** 15-5PH Precipitation hardening stainless steel, electrochemical behavior, acidic solution environments

### 1. INTRODUCTION

Precipitation hardening (PH) martensitic stainless steels like 15-5PH are widely used in the aircraft industry or offshore technologies as structural material, where a balanced combination of high tensile strength and good corrosion resistance. However, the corrosion resistance of 15-5PH martensitic stainless is still an issue due to its mechanical properties main source form the precipitation phase and low lath martensite formed during heat treatment[1,2,3].

Previous investigation works about the behavior of 15-5PH focused on its phases transformation, fracture toughness, fatigue performance, surface integrity et al.[4,5,6,7]. As a high strength stainless steel, the anti-corrosion properties were also characterized by researchers or

companies. A.Abad found that corrosion pitting was caused by the electrical conduction from the power supply to the pieces of 15-5PH at H1025 aging stainless steel in the presence of tap water at 71°C. The chlorinated medium attacked the  $\text{Cr}_2\text{O}_3$  protective layer of the material, and the electrical current rapidly corroded the metal and created the pits[8,9]. X.L. Zhou studied 15-5PH aging at H925, and results showed that the electrochemical impedance magnitude and the impedance module declined with the immersion time. One time constant appeared in EIS spectrum first, then two time constant as the immersion continued. The Scanning Kelvin Probe (SKP) results indicated that the anodic and cathodic areas alternated constantly with distinct character of localized corrosion[10]. Moreover, the pH and  $\text{Cl}^-$  concentration of solutions significantly affect the corrosion resistant on the stainless steel[11,12,13].

Up to now, there is few publication about the passivity and passivity film properties as well as the pitting corrosion behavior of 15-5PH steel either in the acid solutions or in the chloride ions solution[14,15]. This paper mainly studies the effects of pH and chloride ions on the electrochemical corrosion behavior of 15-5PH steel in 0.5M  $\text{Na}_2\text{SO}_4$  acid solution by electrochemical measurements, including corrosion potential, polarization curves and electrochemical impedance spectroscopy(EIS).

## 2. EXPERIMENTAL

The experimental steel was made by vacuum induction melting furnace(VIM) and vacuum self-consuming furnace(VAR) melting, and then rolled into a steel plate 30mm thick. Subsequently the material was subjected to solution annealing at 1040°C for 1 hour, followed by air cooling. Aging was performed by H1025 for 4 hour and by air cooling to the room temperature.

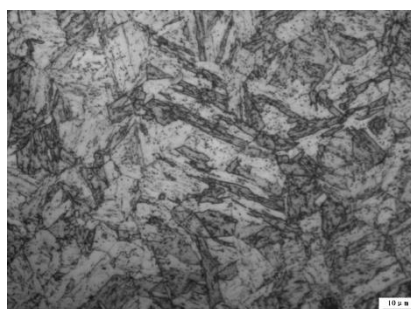


**Figure 1.** Optical micrographs of 15-5PH stainless steel after aging at H1025 for 4hours.

Electrodes used in this work were cut from a 15-5PH steel plate, with a chemical compositions (wt.%): 0.035C, 14.22Cr, 4.69Ni, 3.22Cu, 0.33Nb and balance Fe. The microstructure of the 15-5PH steel was showed in Fig.1, contained lath martensite with thin film shape reverse austenite, and the second phases such as Nb(CN), rich copper phase, and  $\text{M}_{23}\text{C}_6$  precipitates distributing in the steel matrix and grain/lath boundaries[2]. The electrode for the electrochemical measurements has a dimension of 10mm×10mm×3mm and has been embedded in an epoxy resin, exposing a working area

of  $1\text{cm}^2$ . The working surface was ground subsequently up to 1500 grit SiC paper, polished with  $0.1\mu\text{m}$  alumina polishing powder, degreased with alcohol, cleaned in water, and then dried in warm air. cleaned with distilled water and acetone, and dried in cold air. The test solution was  $0.5\text{M}(\text{Na}_2\text{SO}_4+\text{H}_2\text{SO}_4)$  solution [16,17], and prepared with distilled water and analytic grade reagents. The pH of the solution was adjusted by  $\text{H}_2\text{SO}_4$ . The chloride ions concentration contained in the solution was 1%, 3.5%, 5% weight, respectively adjusted by adding NaCl.

The electrochemical measurements were carried out by using a VMP3 electrochemical cell. While the 15-5PH steel electrode was used as working electrode, a platinum wire as the counter electrode and a saturated calomel electrode (SCE) as the reference electrode. The volume of the cell was 500ml. Prior to the test, the steel electrode was processed by cathode polarization at  $-1V_{\text{SCE}}$  for 5 minutes to remove the air-formed oxide film, and then relaxed for 30 minutes to allow the electrode to reach a steady state. The potentiodynamic polarization measurement was carried out at the potential scanning rate of  $0.5\text{mV}\cdot\text{S}^{-1}$ . The EIS measurement was conducted at corrosion potential, over the frequency range of 100kHz to 10mHz, using a  $10\text{mV}_{\text{SCE}}$  sinusoidal potential modulation. All the tests were carried out at room temperature.

The composition of the surface film was analyzed by XPS (ESCALAB 250 of thermo Fisher make), with an Al K of thermo Fisher make), with an Al K $\alpha$  ( $h\nu=1486.6\text{eV}$ ) operated at 150W.

Furthermore, the steel electrode was polarized at  $0.5V_{\text{SCE}}$  in the pH5 solution for 5h. The electrode was then cleaned with distilled water and dried, ready for XPS characterization. Consider the possible oxidation in air, a 9 nm passive film on the electrode was sputtered using a 3kV,  $1\mu\text{A}$   $\text{Ar}^+$  ion beam. The charge shift of the spectra was corrected the C1s peak

### 3. RESULTS AND DISCUSSION

#### 3.1 Effect of solution pH

##### 3.1.1 Potentiodynamic polarization

The polarization curves of 15-5PH steel aging at H1025 for 4 hours was measured in  $0.5\text{M}(\text{Na}_2\text{SO}_4+\text{H}_2\text{SO}_4)$  solution at pH(1,3,5) values respectively was show in Fig.1. It is obvious that the pH affects the electrochemical corrosion behavior of 15-5PH steel, the corrosion potential ( $E_{\text{corr}}$ ) and current density ( $i_{\text{corr}}$ ) in pH acid solution, respectively for  $-392\text{mV}_{\text{SCE}}$  and  $3.875\mu\text{A}$  (pH1),  $-342\text{mV}_{\text{SCE}}$  and  $1.359\mu\text{A}$  (pH3),  $-222\text{mV}_{\text{SCE}}$ ,  $0.103\mu\text{A}$  (pH5). As shown in Fig.2, the polarization curves were divided into four parts: (1) below the "a" point of cathodic area. When at pH 1, the hydrogen reduction is the main cathode reaction [18]. When the pH increases to 3 and 5, considering the solution containing oxygen, the main reduction reaction of cathodic oxygen reduction reaction [19]. (2) In the area of anodic dissolution (a ~ b), the active dissolution current density increases with potential rendering index, until to the maximum critical to blunt electricity  $i_{\text{max}}$ ,  $16.032\mu\text{A}/\text{cm}^2$  (pH=1),  $6.902\mu\text{A}/\text{cm}^2$  (pH=3),  $1.967\text{A}/\text{cm}^2$  (pH=5). The elements of Fe, Cr, Ni, Cu rapid dissolution was the main

cause of the anode current density increase.(3)The section (b~d) was stable passivity section. Within the range(b~c), the sample surface formed the insoluble passivity film such as Fe<sub>3</sub>O<sub>4</sub>, Cr<sub>2</sub>O<sub>3</sub> etal.

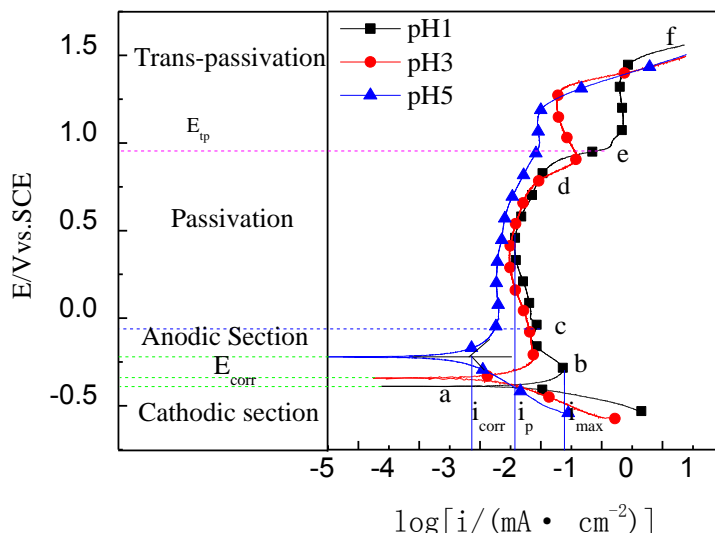
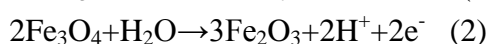
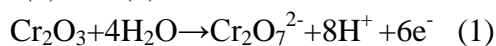


**Figure 2.** The polarization curves of 15-5 PH steel in 0.5M Na<sub>2</sub>SO<sub>4</sub> acid solutions with different pH at room temperature.

Which case of current density with the increase of potential rapidly reduced, the passive current *i<sub>p</sub>* is respectively 7.550μA(pH1),3.006μA(pH3),1.963μA(pH5).As the pH value increases, the15-5 PH steel corrosion potential rises and so does the trans-passivation potential, leading to the enlarge of the passivity potential interval section and proving that the 15-5 PH steel corrosion resistant property was enhanced with the increase of pH value. The corrosion resistance of stainless steel is due to the double oxide film formed on the surface, which is insoluble in acid or alkali solution. The oxide film inner mainly contains chromium oxide, but the outer with iron oxide[20,21]. The corrosion resistant property depends on the quality of the passive film, such as the chemical composition stability of the passive film and its thickness effected by the pH value[22].The section (d~e~f) is the trans-passive section, the trans-passivity and the oxygen evolution is possibly due to the high over-potential. When the potential is above 1.2 V<sub>SCE</sub>, the oxygen evolution reaction leads to the current density increases. The passivity film damage was caused by the nucleation pitting. As the pitting extended in terms of count and depth, the corrosion current density increases accordingly.

It is acceptable that the chromium oxide dissolved to form high valence chromium compound based on the reaction(1).When the potential is above " f " point, the passivation film of sample surface continues to dissolve , such that the iron and chromium elements dissolved into high valence ion in the solution based on reaction(2) and (3).



3.1.2 EIS measurements

EIS is usually used to study metal corrosion because it is capable of manifest various reaction process[23]. The Fig.2 shows the EIS obtained with the 15-5PH steel in 0.5M Na<sub>2</sub>SO<sub>4</sub> acid solution with various pH. The Nyquist curves are shown in Fig.2a, at different pH(1,3,5), the plots are characterized one time constants, a high frequency capacitive loop, which is a typical feature of the iron dissolution in acid solution. The radius of capacitive loop is enlarged as pH value increases, about twice magnitude the radius of capacitive loop of pH(3,5) were pH1, the radius of the semicircle is related to the charge-transfer resistance[24,25], which coincides with the polarization curves in Fig.2. The Bode diagram is shown in Fig.3a, the curves are divided into three parts: ( I ) the section of high frequency(1k-100kHz), where the phase angle close to zero degree, it indicates that the impedance of solution plays dominant role, and the values close to zero; ( II ) medium frequency section(1000-1Hz), the phase angle reaches the maximum value, which is the typical characteristic of capacitive loop; ( III ) low frequency section(0.01-1Hz), the “Z” value represents the corrosion reaction impedance.

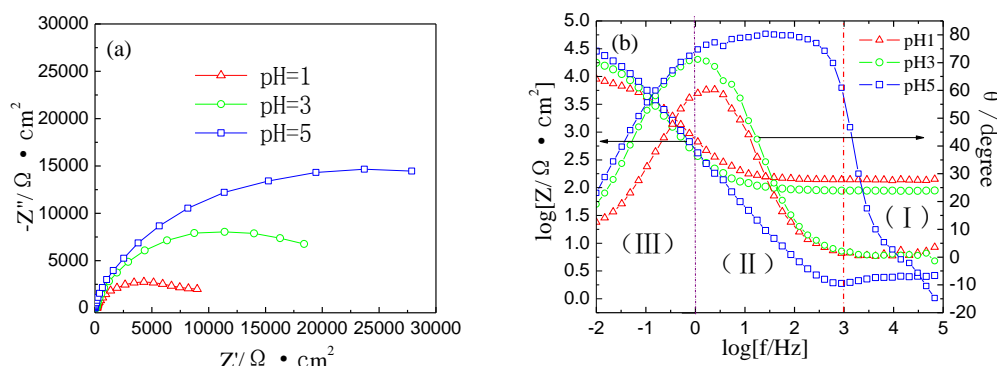


**Figure 3.** Electrochemical impedance of 15-5 PH steel in 0.5M Na<sub>2</sub>SO<sub>4</sub> acid solutions at different pH at open circuit potential. The diagram “a” is Nyquist plots and “b” was Bode plots.

The equivalent circuit model for the EIS data fitting at various pH acid solution is shown in Fig.3, and the fitted results are given in Table 1, where R<sub>s</sub> is the solution resistance, R<sub>f</sub> is the ions pierce in passivity film resistance, R<sub>ct</sub> is the electric double layer capacitance of capacitive resistance. Constant phase element(CPE) is used to consider the frequency independent phase shift between an applied AC potential and its current response. Its admittance, “Y” is defined by Y=Y<sub>0</sub>(jω)<sup>n</sup>[26], where “Y<sub>0</sub>” and “n” are the CPE constant and exponent, respectively, and the “ω” is the angular frequency is rad s<sup>-1</sup>(ω=2πf), and j<sup>2</sup>=-1 is an imaginary number. It might be derived from Table1 that the R<sub>ct</sub> and R<sub>f</sub> increase with the pH value, which coincides with the polarization curves shown in Fig.1. The increase of R<sub>f</sub> indicates that the increase of pH value is of benefit to the growth of passive film and enhances the ability of prevent substrate dissolution.

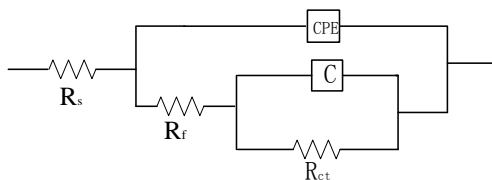


**Figure 4.** The electrochemical equivalent circuit used for simulation of impedance date of 15-5PHsteel electrodes in 0.5MNa<sub>2</sub>SO<sub>4</sub> at different pH acid solution.

**Table 1.** Electrochemical impedance matching data of 15-5 PH steel in acidic solution

pH	R <sub>s</sub> /Ω·cm <sup>2</sup>	Y <sub>0</sub> /(Ω <sup>-1</sup> ·cm <sup>-2</sup> ·S <sup>n</sup> )	n	R <sub>f</sub> /Ω·cm <sup>2</sup>	C/μF·cm <sup>-2</sup>	R <sub>ct</sub> /Ω·cm <sup>2</sup>
1	7.84	6.67E-4	0.85	5034	3.48E-3	5076
3	19.63	5.02 E-4	0.88	2.08E4	1.46E-3	6772
5	20.45	4.87 E-4	0.91	3.52E4	4.31E-3	12080

3.2. Effect of Cl<sup>-</sup> on the passive film

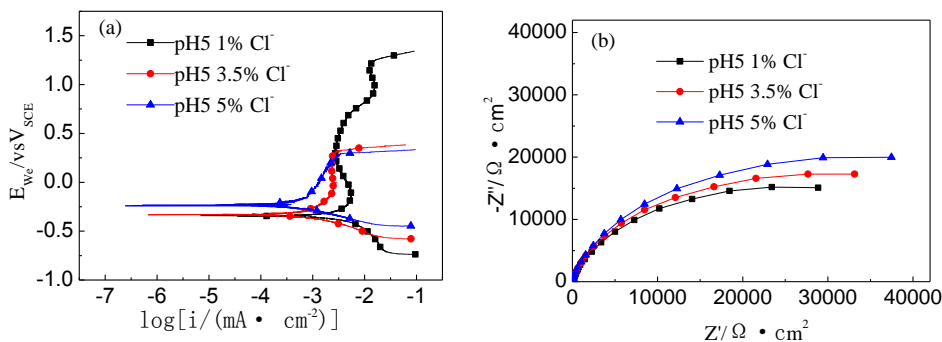


**Figure 5.** The potentiodynamic polarization curves and Nyquist plots of 15-5PH steel in 0.5MNa<sub>2</sub>SO<sub>4</sub>acid solutions at pH5with different chloride concentration at open circuit potential.

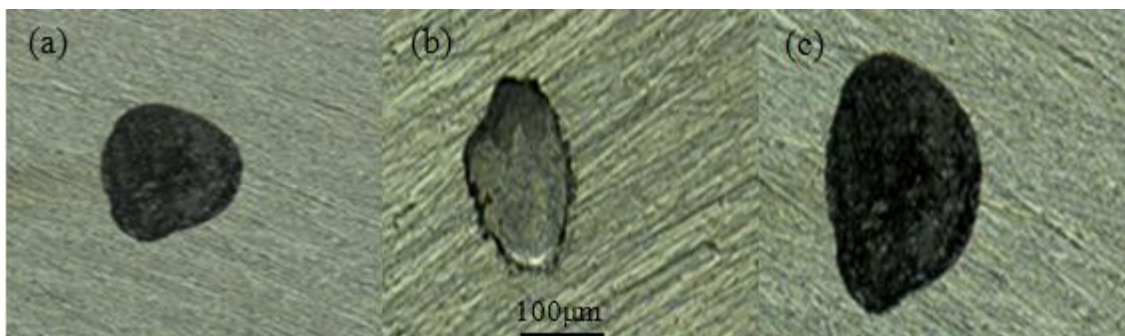


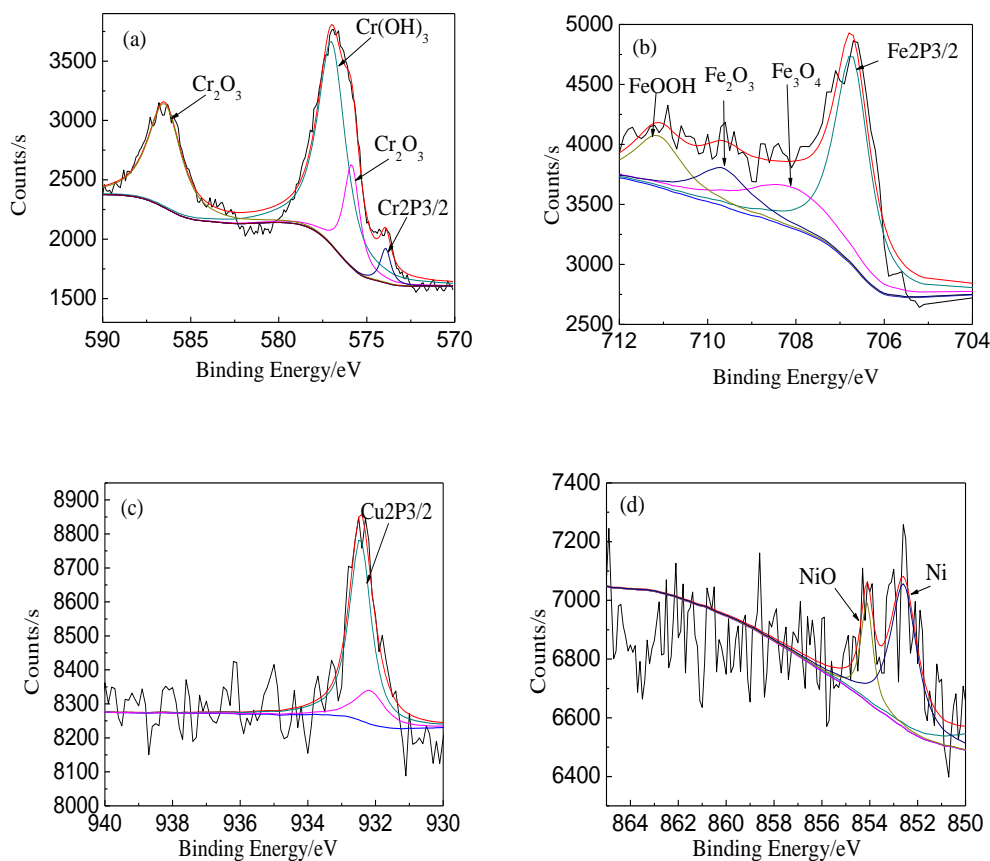
**Figure 6.** SEM morphologies of the corroded surface of 15-5PH after potentiodynamic polarization scan (a) at pH 5 with 1%Cl<sup>-</sup> (b) at pH 5 with 3.5% Cl<sup>-</sup> (c) at pH 5 with 5%Cl<sup>-</sup> added in 0.5 M (Na<sub>2</sub>SO<sub>4</sub>) solution.

The Figure 5(a) shows the polarization curves and Nyquist diagrams measured in pH5 solution at different concentrations of  $\text{Cl}^-$ . As seen from the curves, the addition of  $\text{Cl}^-$  increased the pitting potential and the passive region decreased, with 5% chloride added, the passivity region disappeared. Thus, the electrode is more active in the solution of high chloride than of low chloride. The radius of the capacitive semicircle of Nyquist diagram increases with the concentration of chloride ions.

Thus, the electrode is more active in the high chloride-containing solution than that in low chloride environment. The effect of chloride ions on corrosion of 15-5PH steel was confirmed by SEM observation. As shown in Fig.6, in solution pH 5, 1% chloride ions, very little corrosion pit were formed on the electrode surface, implying that the trans-passivity is mainly due to the oxygen evolution. However, when  $\text{Cl}^-$  up to 3.5%, some hemispherical pits are observed. The corroded surface contained corrosion product around pits.

### 3.3 XPS characterization of the passive film

The chemical composition of the passive film plays an important role in the corrosion resistance properties of 15-5PH stainless steel. The chemical composition of passive film formed at  $0.5V_{\text{SCE}}$  in  $0.5\text{M Na}_2\text{SO}_4$  acid solution of pH5, and was assessed by XPS. and The corresponding spectra are shown in Fig.5. The XPS peaks are deconvoluted on the basis of chemical shifts of respective spectra for the detected element, with the same method as used by literature[27].



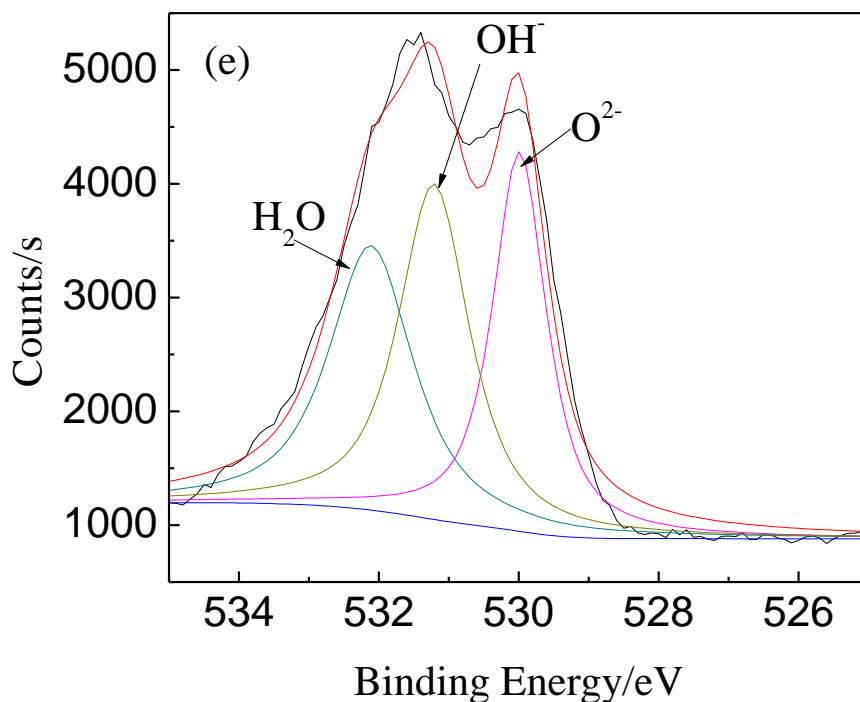


**Figure 7.** The detailed XPS spectra of  $\text{Cr}2\text{P}_{3/2}$ ,  $\text{Fe}2\text{P}_{3/2}$ ,  $\text{Cu}2\text{P}_{3/2}$ ,  $\text{Ni}2\text{P}_{3/2}$ ,  $\text{O}1\text{s}$  of the passive films formed on 15-5PH after polarization at open circuit potential in 0.5M  $\text{Na}_2\text{SO}_4$  acid solution at pH5 for 2h.

In Fig. 7 the high resolution spectra of  $\text{Cr}2\text{P}_{3/2}$ ,  $\text{Fe}2\text{P}_{3/2}$ ,  $\text{Cu}2\text{P}_{3/2}$ ,  $\text{Ni}2\text{P}_{3/2}$  and the  $\text{O}1\text{s}$  were observed. After the background subtraction based on the method suggested by Shirley[28], the XPS results are separated into contributions of the different oxidation states by a fit procedure described in the previous papers [29,30]. Some primary constituents in the film include  $\text{Cr}(\text{III})$ ,  $\text{Fe}(\text{II})$ ,  $\text{Fe}(\text{III})$ ,  $\text{Cu}(0)$ ,  $\text{Ni}(\text{II})$ . In particular, the  $\text{O}1\text{s}$  peak is decomposed into the one at 530.3eV corresponding to  $\text{O}^{2-}$ , and the one at 532.0eV corresponding to  $\text{OH}^-$ . The  $\text{Fe} 2\text{P}_{3/2}$  spectra are fitted with four peaks: 706.7eV corresponding to the metallic state, and the others (708.3eV, 709.4eV and 711.0eV) corresponding to  $\text{Fe}_3\text{O}_4$ ,  $\text{FeO}$  and  $\text{Fe}_2\text{O}_3$ , respectively. The decomposition of  $\text{Cr}2\text{P}_{3/2}$  spectra reveals that there are three constituents representing metallic state  $\text{Cr}$ (at 574.1eV),  $\text{Cr}(\text{OH})_3$ (at 577.3eV),  $\text{Cr}_2\text{O}_3$ (at 576.4eV). The  $\text{Cr}$ ,  $\text{Fe}$  and their oxides in the passive film were also observed by the others. The  $\text{Fe}2\text{P}_{3/2}$  spectra exhibits a stronger signal than the  $\text{Cr}2\text{P}_{3/2}$  spectra, which indicates that the primary constituents of the passive film are iron oxides. The  $\text{Cu}2\text{P}_{3/2}$  spectra was fitted with one peak at 932.6eV corresponding to the metallic state. The  $\text{Ni}2\text{P}_{3/2}$  was fitted with two peaks: 852.6eV corresponding to the metallic state and 854.1eV corresponding to  $\text{NiO}$ .

The XPS results demonstrate that several metal oxides and hydroxides are formed on the steel surface. The primary constituents of the passive film are iron and chromium oxides[31].



#### 4. CONCLUSIONS

(1) At pH(1, 3, 5), the corrosion resistant of 15-5PH in 0.5M(Na<sub>2</sub>SO<sub>4</sub>) acid solution was enhanced, the corrosion current density ( $i_p$ ) was reduced, and the passivity region increases. At pH 1, the hydrogen depolarization reaction was the main cathodic reduction process, with pH value increasing, the oxygen content increases, and thoxxygen was major depolarization of the cathode reaction.

(2) In the chloride acid solution at pH5, the 15-5PH steel pitting potential declined with the chloride ion concentration increasing. When chlorine ion concentration was up to 5%, the anode dissolution was the main reaction.

(3) The passive film of 15-5PH stainless steel formed in the 0.5M Na<sub>2</sub>SO<sub>4</sub> acid solution, predominantly contained Cr-oxides, Ni-oxides, Fe-oxides and Cu species.

#### ACKNOWLEDGEMENTS

This work is supported by the National Natural Science Foundation of China (No.51171023) and the Beijing Municipal Commission of Education.

#### References

1. Z.B.Liu, J.X.Liang, Z.Y.Yang, *Acta Aeronaut. Astronaut. Sin.*, 31(2011)119.
2. H.R.Habibi, B J guirani, *Mater.A Sci.*, 338 (2002) 142 .
3. G.X.Ting, R.W.Bing. *Heat Treat. Met.*,38(2013) 119.
4. L.J.Kai, M. Coret, A. Combescure, *Eng. Fract. Mech.* ,96 (2012) 328.
5. M.A.Shehid,K.Mahmodieh,K.Mori, *Eng. Failure Anal.*, 14(2007) 626.
6. K. J. Abhay, K. S.Kumar, P.P. Sinha, *Eng. Failure Anal.*,17(2010) 1195.
7. A. M.delin,F.Valiorgue, *Proce.Sci.* ,19 (2011) 270.
8. A.Abad,M.Hahn,O.S.Es-Said, *Eng. Failure Anal.*,17(2010) 208.
9. S.P. Brühl,R.Charadia,S.Simison,*Sur.Coat.Technol.*, 204(2010) 3280.
10. Z.X.liang,N.Lun, *J. Chin. Soc. Corros. Prot.*, 32(2012) 427.
11. J.D.Kim,S.I.Pyun, *Electrochim. Acta.*, (40)1995-1863.
12. C.T. Liu, J.K. Wu, *Corros. Sci.*49(2007) 2198.
13. M.J. Carmezim, A.M. Simoes , M.F. Montemor, *Corros. Sci.* ,47(2005)581.
14. D.S.zou, M.Pagitsas, *J. Electroanal. Chem. Interfacial Electrochem.*,304(1991)171.
15. S.S.Abd ElRehim, A.A.ElBasosi, M.M. Osman, *J. Electroanal. Chem.*348(1993)99.
16. J. Bockris,D.Drazic,A.R.Despic, *Electrochim. Acta.*, (1961)325.
17. A.A. Abdul Azim, S.H. Sanad, *Electrochim. Acta.*,(1972)1699.
18. A.Davydov, K .V. Rybalka, L. A. Beketaeva, *Corros. Sci.* ,47(2005) 195.
19. M.Stratmann,J.Müller, *Corros. Sci.* ,36(1994)327.
20. 20 . X. Q.Cheng, Z. C. Feng, C. T. Li, *Electrochim.Acta*,(2011) 5860.
21. Metikoš-HukovićM,Babić, *Corros. Sci.*,49(2007)3570.
22. S.E. Ziemniak, M. Hanson,*Corros. Sci.*,44(2002)2209.
23. M. Itagaki, T. Suzuki, K. Watanabe, *Corros. Sci.*,40(1998)1255.
24. K.Jüttner, *Electrochim. Acta.*,35(1990)1501.
25. T.Paskossy, *J.Electroanal. Chem.*,364(1994)111.
26. G.J. Brug, A.L Eeden, M.S.Rehbach, *J.Electroanal.Chem.*,176(1984) 275.
27. J.Chastain, Handbook of X-ray Photoelectron Spectroscopy, *Physical Electronics Inc*,1995.

28. D.A. Shirley, *Phys. Rev. B* 5 (1972) 4709.
29. S. Haupt, C. Calinski, U. Collisi, *Surf. Interface Anal.*,9(1986)357.
30. J.F.Moulder, Handbook of X-ray Photoelectron Spectroscopy, Perkin-Elmer Corporation, USA, 1992.
31. H. Jung, A. Alfantazi, *Electrochim. Acta.*,55(2010)865.

© 2015 The Authors. Published by ESG ([www.electrochemsci.org](http://www.electrochemsci.org)). This article is an open access article distributed under the terms and conditions of the Creative Commons Attribution license (<http://creativecommons.org/licenses/by/4.0/>).